THE JOURNAL OF PHYSICAL CHEMISTRY Letters

LETTER

pubs.acs.org/JPCL

Panchromatic Sensitized Solar Cells Based on Metal Sulfide Quantum Dots Grown Directly on Nanostructured TiO_2 Electrodes

Antonio Braga,[†,‡] Sixto Giménez,[†] Isabella Concina,[‡] Alberto Vomiero,[‡] and Iván Mora-Seró*[,†]

[†]Photovoltaic and Optoelectronic Devices Group, Departament de Física, Universitat Jaume I, 12071 Castelló, Spain

[‡]Department of Physics and Chemistry for Materials and Engineering and CNR-IDASC SENSOR Lab, Brescia University, Via Valotti 9, 25133 Brescia, Italy

Supporting Information

ABSTRACT: The use of narrow band gap semiconductors such as PbS may expand the light absorption range to the near-infrared region in quantum-dot-sensitized solar cells (QDSCs), increasing the generated photocurrent. However, the application of PbS as a sensitizer in QDSCs causes some problems of stability and high recombination. Here, we show that the direct growth of a CdS coating layer on previously deposited PbS by the simple method of successive ionic layer adsorption and reaction (SILAR) minimizes these problems. A remarkable short-circuit current density for PbS/CdS QDSCs is demonstrated, ~11 mA/cm^2, compared to that of PbS QDSCs, with photocurrents lower than 4 mA/cm^2, using polysulfide electrolyte in both cells. The cell efficiency reached a promising 2.21% under 1 sun of simulated irradiation (AM1.5G, 100 mW/cm^2). Enhancement of the solar cell performance beyond the arithmetic addition of the efficiencies of the single constituents (PbS and CdS) is demonstrated for the nanocomposite PbS/CdS configuration. PbS dramatically increases the obtained photocurrents, and the CdS coating stabilizes the solar cell behavior.

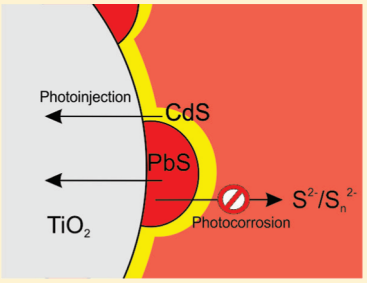

SECTION: Energy Conversion and Storage

Sensitized solar cells[1] have introduced new concepts for the development of photovoltaic devices. Nanoscale light absorbers can quickly separate the photogenerated carriers into two different media. This fact allows the use of low-cost materials and, subsequently, a significant cost reduction compared to other photovoltaic technologies. One of the current challenges of sensitized solar cells is expanding the light absorption range from the visible to the near-infrared (NIR) region of the solar spectrum in order to maximize the generated photocurrent. The absorption region of molecular dyes, commonly used in dye-sensitized solar cells (DSCs), is limited. On the other hand, an intensive research effort is currently being carried out on the use of semiconductors as light-absorbing materials for this kind of solar cells.[2−6] Semiconductor materials can absorb all photons with energies higher than their band gap, E_g, while molecular dyes can only absorb light photons within a more or less broad band corresponding to their molecular transitions. Semiconductors with E_g in the infrared (IR), such as PbS with E_g = 0.41 eV,[7] have attracted enormous interest as sensitizers because they can allow extension of the absorption band toward the NIR part of the solar spectrum. Recently, the use of PbS[8] and PbSe[9] colloidal quantum dots in Schottky solar cells has demonstrated the potential of these materials for solar energy conversion, obtaining remarkably high photocurrents (>21 mA/cm^2).[8] The performance of these systems has also been increased by the use of TiO_2 as an electron-selective contact in a depleted heterojunction colloidal quantum dot solar cell configuration.[10] In these configurations, the colloidal QD layer acts simultaneously as a light absorber and hole transporter.

Conventional sensitized solar cells require a simpler manufacturing process compared to that of the previous examples. These cells possess a thin layer of the light absorber and a different hole conductor material. When these cells use semiconductor QDs as light absorbing material they are commonly called quantum dot sensitized solar cells (QDSCs). However, bulk PbS exhibits three problems for its use in sensitized solar cells; (i) due to its low E_g, the maximum theoretical efficiency is far below 33%, reported for an absorber with a band gap of 1.4 eV,[11] (ii) Its conduction band (CB) is located at lower energy compared to that of TiO_2 (see Figure 1a), commonly used as electron-transporter material in sensitized cells, and consequently, the electron injection from PbS into TiO_2[12] is suppressed, and (iii) PbS is not stable with redox couples as iodine or polysulfide.[13] The first two problems can be circumvented by reducing the size of PbS particles below the Bohr's radius, where the quantum confinement regime is reached. PbS QD present higher E_g than bulk PbS, and also, the energy position of their CB is up-shifted, allowing the fast electron injection into TiO_2;[10,12,14] see Figure 1a. The instability of PbS in polysulfide electrolyte can be overcome using adequate synthetic routes, as demonstrated in the present study. We report the

Received: January 4, 2011
Accepted: February 1, 2011

   dx.doi.org/10.1021/jz2000112 | J. Phys. Chem. Lett. 2011, 2, 454–460

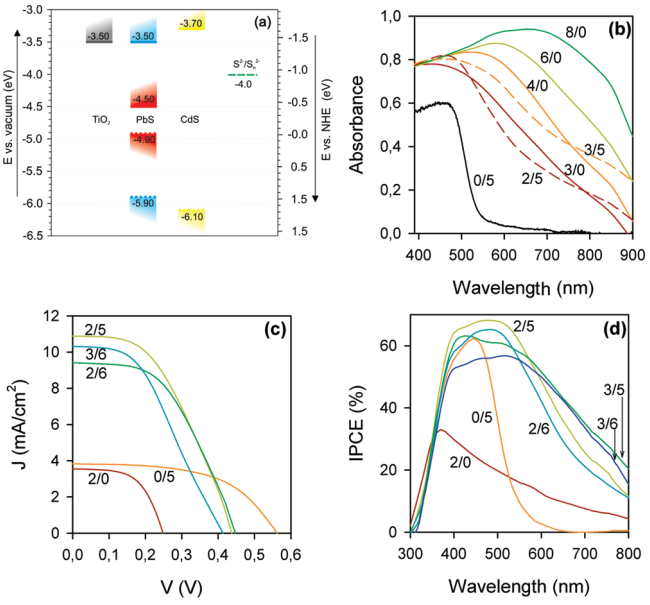

Figure 1. (a) Position of the conduction band (CB) and valence band (VB) of TiO_2 (considering pH = 13, the polysulfide pH),[25] bulk PbS and bulk CdS (calculated at pH = 7),[24] and an S^{2-}/S_n^{2-} redox level.[26] Solid lines mark the bottom of the CB, and dotted lines the top of the VB. For PbS, red color is used for bulk material, while blue color is used for a QD with the CB coincident with the TiO_2 CB. The diagram can allow qualitative interpretation of the charge injection process, despite the small variations that can exist between the analyzed materials and data in the literature. (b) Absorption spectra of QD-sensitized electrodes. (c) $J-V$ curves of QDSCs under 1 sun of illumination (AM 1.5G). (d) IPCE spectra of QDSCs. QDSCs are denoted as X/Y, where X and Y are the number of SILAR cycles for PbS and CdS, respectively.

in situ deposition of PbS and CdS QDs by a successive ionic layer adsorption and reaction (SILAR) process onto a mesoporous TiO_2 photoanode. The optimized synergistic combination of these materials led to a stable panchromatic solar cell using polysulfide as the electrolyte. Moreover, we obtained a remarkable improvement of the short-circuit current density, close to 11 mA/cm^2, compared to that of single-material deposition, with photocurrents lower than 4 mA/cm^2. The cell efficiency reached a promising 2.21% under 1 sun of simulated irradiation (AM1.5G, 100 mW/cm^2). To the best of the authors' knowledge, this efficiency is the highest one reported in the QDSC configuration either with PbS or CdS as the light-absorbing material.

Considering PbS and CdS QDs, the most promising QDSC energy conversion efficiencies (under 1 sun of illumination) was obtained when the QDs were grown by SILAR. Regarding the hole transport material, 1.84%[15] conversion efficiency has been obtained using CdS and I^-—I_3^- as the electrolyte. However, corrosion of CdS takes place with the I^-—I_3^- electrolyte, unless the semiconductor light absorber is protected with a coating material such as TiO_2.[2] Using this coating, an efficiency of 1.24% was obtained for CdS QDSCs grown by chemical bath deposition.[16] Using spiro-OMeTAD, a solid hole conductor, a 1.46% efficiency for PbS and 0.80% for CdS has been achieved.[13] Particularly, when CdS is combined with the SQ1 dye, the efficiency increases up to 1.20%.[13] The CuSCN hole conductor led to an efficiency of 1.3%.[17] Lower efficiencies have been reported for both PbS and CdS using a Co-based redox due to the diffusion limitation of this electrolyte.[18] In all cases, the reported photocurrents for nanoporous cells based on PbS, J_{sc}, lay below 5 mA/cm^2; which seriously limits the final efficiency of the device. In addition, it is interesting to note that the use of TiO_2 nanotube arrays increases the performance of CdS QDSCs deposited by SILAR.[19]

It has been shown that polysulfide (S^{2-}/S_n^{2-}) electrolyte leads to the highest reported photocurrents for QDSCs.[20,21] PbS is stable with spiro-OMeTAD and Co-redox as hole-conducting systems,[13,18] but unfortunately, it is not stable with polysulfide.[13,22] Conversely, CdS is stable with polysulfide,[2,20] although the efficiency of CdS-based QDSCs is limited by its relatively wide band gap. The stabilization of PbS in polysulfide electrolyte by coating PbS QDs with a CdS capping layer can offer an elegant and multifunctional solution to the problem. The synergistic combination of both semiconductors leads to a dramatic increase in photocurrent and efficiency for the photovoltaic devices. Additionally, the solar cells are stable with polysulfide electrolyte. Previous studies on the PbS/CdS system have been reported, showing relatively poor photoconversion efficiency. Lee et al. obtained an efficiency of 0.1% using a PbS/CdS/ZnS TiO_2-sensitized electrode, using polysulfide electrolyte and SILAR deposition for PbS (five cycles), CdS (one cycle), and ZnS (one cycle).[23] Vogel et al. reported SILAR preparation of PbS on nanoporous TiO_2 and the resulting cells in the sulfide/sulfite electrolyte, obtaining a significant incident photon to current efficiency (IPCE) of 70% using a 460 nm excitation wavelength but in a three-electrode configuration and employing an electrolyte with lower recombination than the polysulfide.[24] Yang et al. reported a 1.6% efficiency at very low light power density, corresponding to 1 mW/cm^2 under a 660 nm excitation wavelength.[22] It is important to point out that the last two references also observe a significant increase of the stability of PbS after CdS coating.[22,24]

In the present study, PbS and CdS QDs have been in situ deposited by the SILAR process onto TiO_2 mesoporous substrates. Several sensitizing configurations have been analyzed, including the deposition of "only PbS" or "only CdS" and the hybrid system PbS/CdS (first PbS is deposited onto TiO_2 and then CdS). The samples are labeled as X/Y, where X and Y refer to the numbers of PbS and CdS SILAR cycles, respectively. All of the analyzed samples were coated with two cycles of ZnS grown by SILAR; see the Experimental Methods section. It is observed that the electrodes undergo chromatic changes by increasing the number of SILAR cycles. When present, CdS prevents PbS from photochemical corrosion processes.[22]

The effect of the number of SILAR cycles on the optical properties of PbS and CdS QD-sensitized TiO_2 is illustrated by the UV—Vis absorption spectra (Figure 1b). Increasing the number of cycles leads to a progressive aggregation of the QDs and a concomitant shift of the absorption feature toward higher wavelengths. A significant red-shift (from ~515 to ~655 nm) is observed for the absorption peak of the only PbS electrodes (Figure 1b), corresponding to samples 4/0 and 8/0, respectively. Enhanced absorption in the NIR region should increase the amount of photogenerated electrons and, consequently, J_{sc}. However, as it has been commented, the use of PbS sensitizer without any CdS protective layer leads to nonstable cells with polysulfide electrolyte; see below. When CdS is deposited onto PbS, a reduction in the quantum confinement of PbS takes place, leading to an enhancement of the absorption; compare, for example, samples 3/0 and 3/5 in Figure 1b. Consequently, a significant broadening of the IPCE features is observed; see Figure 1d.

dx.doi.org/10.1021/jz2000112 |J. Phys. Chem. Lett. 2011, 2, 454–460

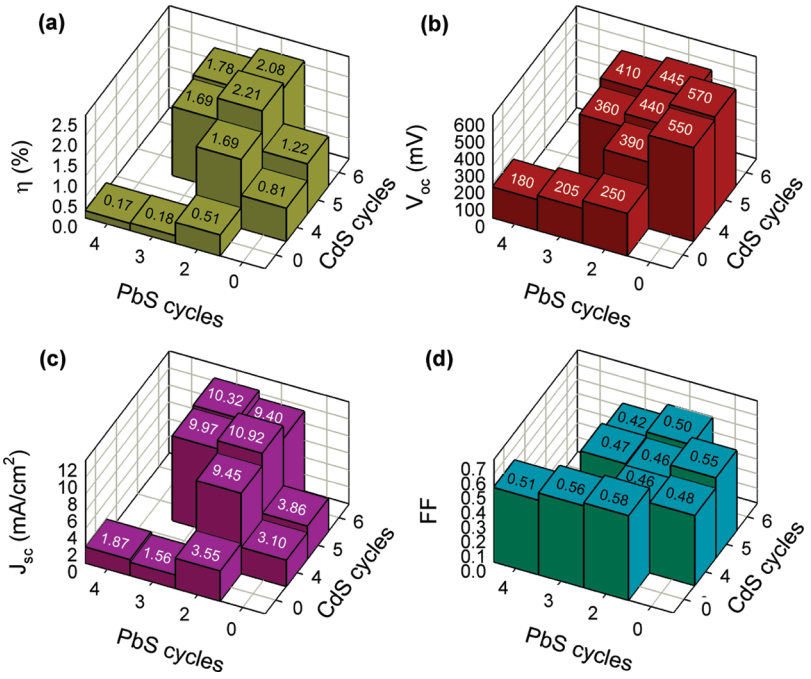

Figure 2. Solar cell parameters depending on the number of SILAR cycles; (a) efficiency (η), (b) open-circuit potential (V_{oc}), (c) short-circuit current density (J_{sc}), and (d) fill factor (FF).

The current density−voltage ($J-V$) curves recorded at full 1 sun of illumination are depicted in Figure 1c. The photovoltaic parameters of the analyzed PbS, CdS, and PbS/CdS cells are reported in Figure 2. Only PbS (2/0) and only CdS (0/5) QDSCs exhibit low photocurrents. The 0/5 sample is characterized by a relatively high open-circuit voltage, V_{oc} = 570 mV. On the other hand, the 2/0 sample presents a very low V_{oc} = 250 mV. Additionally, only PbS solar cells exhibit a nonstable behavior, as we will discuss later, even with a ZnS coating. In contrast, the hybrid samples combining PbS and CdS show an intermediate V_{oc} between those for PbS and CdS QDSCs. However, a remarkable increase in J_{sc} is observed (see Figure 1c), leading to a dramatic improvement in efficiency (see Figure 2a). The photocurrent enhancement is due to the extension of the light absorption region into the red and NIR, as derived from the IPCE spectra (see Figure 1d).

In addition to the increase of the cell performance for the hybrid configurations, the photochemical stabilization of PbS takes place with the presence of the CdS coating. Figure 3 shows the evolution of J_{sc} with time for a PbS sample (2/0) and for the hybrid sample (2/5), which is the best operating cell in terms of cell efficiency (Figure 2a). Aiming at a better comparison between cells, the photocurrent of cell 2/0 has been normalized to that of sample 2/5, denoted as $2/0_{nor}$ in Figure 3. While the cell 2/5 shows a stable behavior, taking into account that the cell is not completely sealed (see the Experimental Methods section), cell 2/0 is characterized by a continuous decrease of the current, indicating the progressive degradation of PbS, which we are reasonably attributing to PbS oxidative processes.[22] It is important to note that the stabilization of PbS by CdS coating is obtained when CdS is deposited immediately after completing the deposition of PbS. When some time is left between the deposition of PbS and the subsequent CdS coating, nonstable cells are obtained. This fact reflects the fundamental role of the surface termination on the photochemical properties of the QD

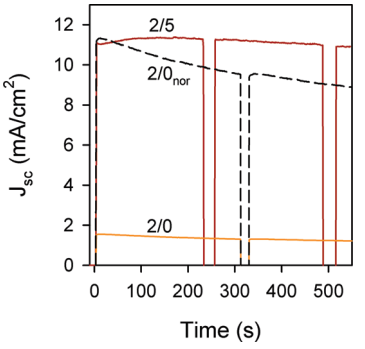

Figure 3. Photocurrent as a function of time comparing an only PbS cell (2/0) with a hybrid PbS/CdS cell (2/5). For the sake of clarity, the maximum photocurrent of the only PbS cell has been normalized ($2/0_{nor}$) to the maximum photocurrent of the hybrid PbS/CdS cell. The rapid decrease and increase of photocurrent observed in the graph corresponds to a light switch off and light switch on, respectively.

absorber. On the other hand, note that the photocurrent reported in Figure 3 for the sample 2/0 is significantly lower than the reported one in Figures 1 and 2 (which is not the case for highly stable sample 2/5) as a consequence, precisely, of this continuous decrease of the photocurrent.

After analyzing the solar cell parameters obtained for the different sensitizing configurations reported in Figure 2, some characteristic trends can be unveiled. V_{oc} increases with the number of CdS SILAR cycles and decreases with the number of PbS SILAR cycles; see Figure 2b. The photocurrent, as has been previously commented, remarkably increases for PbS/CdS hybrids; see Figure 2c. Finally, the FF obtained is around 0.5 for all of the samples; see Figure 2d. The slight differences observed in the FF can be attributed to the different photocurrents; cells with lower photocurrents present higher FF because the voltage drop in the series resistance is lower.

dx.doi.org/10.1021/jz2000112 |J. Phys. Chem. Lett. 2011, 2, 454–460

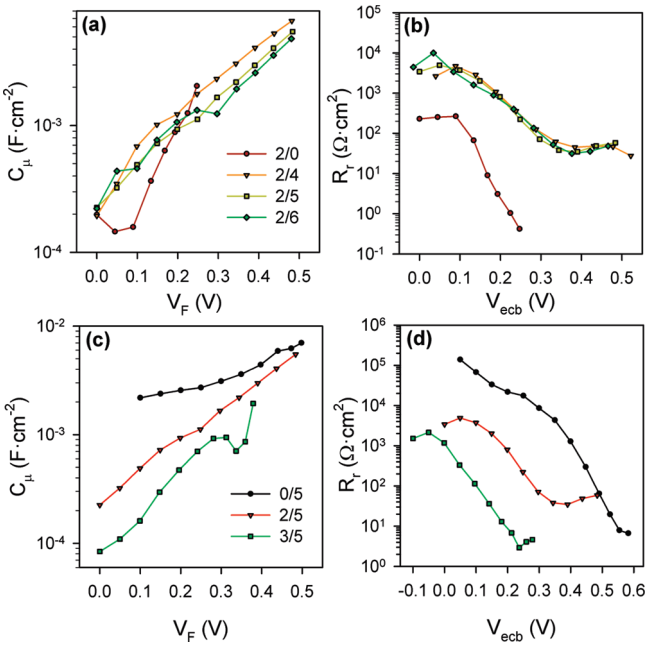

Figure 4. Capacitance and recombination resistance of QDSCs extracted from impedance spectroscopy measurements. (a) Capacitance and (b) recombination resistance depending on the number of CdS SILAR cycles. (c) Capacitance and (d) recombination resistance depending on the number of PbS SILAR cycles. V_{ecb} refers to a common equivalent conduction band shifting the voltage drop in the sensitized electrode, V_F, in order to remove the effect of different positions of the TiO_2 CB among samples.[27]

To better understand these characteristic trends and to examine the physical processes occurring in QDSCs, impedance spectroscopy (IS) characterization has been carried out. Additionally, from the deep understanding of the underlining physical processes, the conversion efficiency of the devices could be boosted. The analysis of the IS spectra of only PbS, only CdS, and hybrid PbS/CdS QDSCs can be carried out by employing the equivalent circuit previously reported to analyze DSCs[28] and QDSCs.[20] Figure 4 illustrates the basic parameters to analyze solar cell performance, the chemical capacitance, C_μ, and the recombination resistance, R_r, for different cell configurations.[29] The chemical capacitance, Figure 4a and c, is plotted against the voltage drop in the sensitized electrode, V_F. V_F is obtained from IS measurements, taking into account the voltage drop at the series resistance, V_s (contacts, transport resistance, counter-electrode), as $V_F = V_{appl} - V_s$, where V_{appl} is the applied voltage.[20,27,30] Only CdS and hybrid PbS/CdS samples show very similar slopes for C_μ, although C_μ is shifted, indicating an upward displacement of the TiO_2 CB with the number of PbS or CdS SILAR cycles. In general, the surface modification of TiO_2 could produce an effect on the band alignment as it has been observed by using molecular dipoles[30,31] or increasing the number of CdSe SILAR cycles.[20] In order to compare the recombination resistance among different samples, this shift has to be removed to exclude the effect of the TiO_2 CB position, representing the different parameters as a function of a common equivalent conduction band, V_{ecb}.[20,27,30] This procedure allows analysis of the recombination resistance (R_r depends on the density of electrons in the TiO_2 CB) on the basis of an equal density of electrons n (i.e., the same distance between the electron Fermi level and the CB of TiO_2). This is carried out by shifting V_F until the chemical capacitance overlaps;[20,27,30] see also Supporting Information S1. Sample 2/0 exhibits a different slope compared to that of the other samples due to the degradation process (see below), and no shift has been considered for this sample.

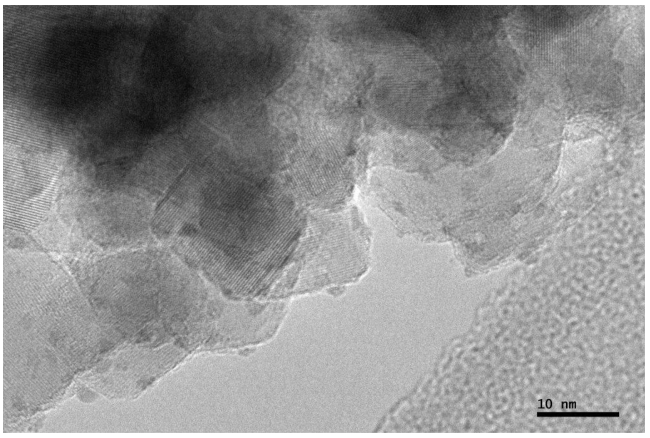

Figure 5. TEM image of a PbS 2/0 sensitized electrode (with no CdS or ZnS coating). The bigger crystalline grains correspond to anatase TiO_2, while the small features on TiO_2 correspond to PbS QDs with sizes between 2 and 3 nm.

Considering R_r for samples with different numbers of CdS SILAR cycles (see Figure 4b), very similar recombination resistances are obtained for hybrid samples independently of the number of CdS cycles. A much lower recombination resistance is obtained for the 2/0 sample. The lower R_r for this sample explains its low V_{oc}; see Figure 2b. On the other hand, the upward shift of the TiO_2 conduction band with the CdS cycles (Figure 4a) is responsible for the increase in V_{oc} observed with the number of CdS cycles (see Figure 2b) as R_r remains unchanged (see Figure 4b). In addition, increasing the number of PbS SILAR cycles (see Figure 4d) leads to a significant decrease of R_r. This fact is responsible for the lower V_{oc} observed as the number of PbS cycles increases (see Figure 2b). The high recombination in PbS cells causes the photoconversion efficiency in these cells to be limited by transport; see Suporting Information S2. This analysis indicates that the nature of the semiconductor light absorber employed in QDSCs dramatically affects the final performance of the device in terms of charge recombination, as is expected.

Figure 5 shows a TEM image of a TiO_2 electrode sensitized with two SILAR cycles of PbS. The PbS SILAR process produces well-separated PbS QDs, as has been also previously reported.[13,23] Due to the mesoporous structure of this electrode, a big portion of the TiO_2 surface remains uncovered. In contrast, a practically complete coverage of the TiO_2 surface can be reached when CdS[17,20,23] or even CdSe are deposited with a high enough number of SILAR cycles.[20] It has been demonstrated that the CdS or CdSe QD light-absorbing layer acts as blocking layer, reducing the recombination in QDSCs.[5,20] In our present study, the low coverage of the TiO_2 surface by PbS undoubtedly contributes to higher recombination rates. However, this is not the main factor because an increase of PbS SILAR cycles enhances the recombination; see Figure 4d. If surface coverage was the only factor contributing to the recombination, an increase of the recombination resistance should be obtained. It has been suggested

dx.doi.org/10.1021/jz2000112 |J. Phys. Chem. Lett. 2011, 2, 454–460

that the catalytic properties of PbS for reducing S_n^{2-} also contribute to enhance the recombination.[23] Moreover, the role of surface states in the recombination process cannot be ruled out.

On the other hand, we have applied the β-recombination model[32] to study the recombination properties of the QDSCs under investigation. In such a model, the recombination rate in sensitized solar cells is proportional to n^{β}, where n is the electron density in the TiO_2 and β is a parameter lower than 1. β values can be extracted from the slope of R_r versus V_F.[29] The obtained values of β for only CdS and hybrid PbS/CdS cells are, in general, slightly lower than 0.5; see Supporting Information S3. Similar values of β have also been observed for CdSe QDSCs.[20] The 2/0 cell exhibits a $\beta = 1.05$. An ideal device presents a $\beta = 1$; higher β values indicate a faster decay of R_r with voltage, providing additional proof of the degradation of only PbS devices.

These two facts clearly reflect the deficient performance of PbS in QDSCs when using polysulfide as electrolyte. The synergistic combination of PbS with CdS provides an stable hybrid sensitizer compatible with polysulfide. Moreover, the efficiency of the hybrid devices is significantly higher than the additive contribution of the efficiencies of each individual component. In this sense, PbS and CdS constitute promising nanocomposite structures with supracollecting properties.[33]

The observed trends for J_{sc} and V_{oc} can be explained from the IPCE spectra together with the analysis of C_μ and R_r. In addition, an excessive amount of light-absorbing material could block the pores in the TiO_2 matrix, leading to a limitation of the photocurrent.[20] Consequently, the optimization of the number of SILAR cycles is a key factor to boost the efficiency of these devices.

The solar cell performance of the devices studied in the present study has been successfully explained through the experimental characterization and the employed models. In agreement, other relevant parameters commonly used in the literature for electron conductivity, lifetime, diffusion coefficient, and small perturbation diffusion length are reported for the analyzed QDSCs as Supporting Information S4 and S5.

To conclude, we have reported efficient and stable panchromatic QDSCs based on metal sulphide semiconductors. The nanocomposite PbS/CdS configuration has been demonstrated to enhance the solar cell performance beyond the arithmetic addition of the efficiencies of the single constituents. PbS dramatically increases the obtained photocurrents, and the CdS coating stabilizes the solar cell behavior. The comprehensive study through IS characterization clearly indicates that the large recombination of the PbS layer limits the cell efficiency, and higher efficiencies should be expected, provided that this recombination is controlled. The design of supracollecting absorbers, based on nanocomposites synergistically integrating different individual constituents, opens an interesting research field in nanotechnology, potentially leading to significant breakthroughs in sensitized solar cell devices.[33]

EXPERIMENTAL METHODS

Quantum Dot Solar Cell Preparation. A standard TiO_2 mesoporous photoanode has been selected as the working electrode because it demonstrated the best operating performance in classical DSC configuration.[34,35] The photoanode structure is based on a double layer of TiO_2 nanoparticles made by a transparent and an opaque thin film of titania paste with nanoparticles of different sizes (20 nm for the transparent layer,18NR-AO Dyesol, and a mixture of 300−400 nm for the layer with enhanced light scattering, WERO4 Dyesol). The photoanodes were deposited by tape casting the pastes onto transparent conducting fluorine-doped tin oxide (FTO) glass substrates (sheet resistance ∼10 Ω/□). Previously, the FTO/glass substrates were coated by a compact layer of spray-pyrolyzed titanium dioxide (∼100 nm thick). Calcination at 450 °C in a muffle and final $TiCl_4$ treatment were carried out before sensitization. The thickness of the mesoporous electrodes was around 14 μm (9 μm of transparent layer and 5 μm of scattering layer), measured by scanning electron microscopy (SEM) with a JSM-7000F JEOL FEG-SEM system, with a dispersion lower than 10%.

The SILAR process has been carried out following the method recently described.[13,15,18] The deposition of PbS and CdS QDs includes the use of two different solutions of metals and sulfide precursors. A 0.02 M methanolic solution of $Pb(NO_3)_2 \times 4H_2O$ was used as the Pb^{2+} source. Similarly, Cd^{2+} ions have been deposited from an ethanolic 0.05 M solution of $Cd(NO_3)_2 \times 4H_20$. The sulfide sources were 0.02 and 0.05 M solutions of $Na_2S \times 9\ H_2O$ in methanol/water (50/50 V/V) for Pb^{2+} and Cd^{2+} ions, respectively. A single SILAR cycle consisted of 1 min of dip-coating of the TiO_2 working electrode into the metal precursors (Pb^{2+} or Cd^{2+}) and subsequently into the sulfide solutions. After each bath, the photoanode was thoroughly rinsed by immersion in the corresponding solvent to remove the chemical residuals from the surface and then dried in air. For the hybrid PbS/CdS samples, the CdS deposition was carried out immediately after PbS deposition.

In order to improve the performance and stability of the solar cells, a ZnS protective coating was deposited on the photoanode after the PbS and/or CdSe sensitization.[5,35,36] The device was finally completed by sandwiching the working electrode with a Cu_2S counter electrode and permeating with polysulfide electrolyte according to ref 7, clamping the sensitized electrode and counter electrode using scotch tape as the spacer. At least two cells have been prepared at each condition for statistical significance with very good reproducibility; see Supporting Information S6.

Photoanode and Solar Cell Characterization. The optical absorption spectra of the photoanodes were recorded at 350−900 nm by a Cary 500 UV−vis Varian photospectroscometer. $J-V$ curves were obtained using a FRA-equipped PGSTAT-30 from Autolab and a Keithley 2612 System SourceMeter. The cells were illuminated using a solar simulator at AM1.5 G, where the light intensity was adjusted with an NREL-calibrated Si solar cell with a KG-5 filter to 1 sun of intensity (100 mW/cm^2). The IPCE measurements have been performed by employing a 150 W Xe lamp coupled with a computer-controlled monochromator; the photocurrent was measured using an optical power meter 70310 from Oriel Instruments. Impedance measurement were carried out with a FRA-equipped PGSTAT-30 from Autolab, applying a 20 mV AC signal and scanning in a frequency range between 400 kHz and 0.1 Hz at different forward applied bias. For TEM measurements, a JEM-2100 electron microscope (JEOL) operated at 200 kV was used.

ASSOCIATED CONTENT

Supporting Information. Correcting the effect of the position of the TiO_2 conduction band, transport versus recombination resistance, calculation of β in PbS, CdS, and PbS/CdS

QDSCs, electron conductivity, lifetime, diffusion coefficient, and small perturbation diffusion length for QDSCs with different numbers of CdS and PbS SILAR cycles. This material is available free of charge via the Internet at http://pubs.acs.org.

AUTHOR INFORMATION

Corresponding Author
*E-mail: sero@fca.uji.es.

ACKNOWLEDGMENT

This work was supported by the Ministerio de Ciencia e Innovación of Spain under the Projects HOPE CSD2007-00007, JES-NANOSOLAR PLE2009-0042, and MAT2007-62982 and by the CARIPLO Foundation under the Contract 2008.2393. S. G. acknowledges the financial support of the Spanish Ministerio de Ciencia e Innovación through the Ramón y Cajal program. The authors want to thank Professor Giorgio Sberveglieri and Professor Juan Bisquert for the fruitful discussions on the topics related to this article, the SCIC of University Jaume I (Spain) for providing the microscopy facilities, and also Sonia Ruiz-Raga for preparing the TOC and Figure 1a.

REFERENCES

(1) O' Regan, B.; Grätzel, M. A Low-Cost High-Efficiency Solar Cell Based on Dye-Sensitized Colloidal TiO_2 Films. *Nature* **1991**, *353*, 737–740.

(2) Hodes, G. Comparison of Dye- and Semiconductor-Sensitized Porous Nanocrystalline Liquid Junction Solar Cells. *J. Phys. Chem. C* **2008**, *112*, 17778–17787.

(3) Kamat, P. V. Quantum Dot Solar Cells. Semiconductor Nanocrystals as Light Harvesters. *J. Phys. Chem. C* **2008**, *112*, 18737–18753.

(4) Rühle, S.; Shalom, M.; Zaban, A. Quantum-Dot-Sensitized Solar Cells. *Chem. Phys. Chem.* **2010**, *11*, 2290–2304.

(5) Mora-Seró, I.; Giménez, S.; Fabregat-Santiago, F.; Gómez, R.; Shen, Q.; Toyoda, T.; Bisquert, J. Recombination in Quantum Dot Sensitized Solar Cells. *Acc. Chem. Res.* **2009**, *42*, 1848–1857.

(6) Kamat, P. V.; Tvrdy, K.; Baker, D. R.; Radich, J. G. Beyond Photovoltaics: Semiconductor Nanoarchitectures for Liquid-Junction Solar Cells. *Chem. Rev.* **2010**, *110*, 6664–6688.

(7) Ratanatawanate, C.; Xiong, C.; Balkus, K. J. Fabrication of PbS Quantum Dot Doped TiO_2 Nanotubes. *ACS Nano* **2008**, *2*, 1682–1688.

(8) Luther, J. M.; Law, M.; Beard, M. C.; Song, Q.; Reese, M. O.; Ellingson, R. J.; Nozik, A. J. Schottky Solar Cells Based on Colloidal Nanocrystal Films. *Nano Lett.* **2008**, *8*, 3488–3492.

(9) Debnath, R.; Tang, J.; Barkhouse, D. A.; Wang, X.; Pattantyus-Abraham, A. G.; Brzozowski, L.; Levina, L.; Sargent, E. H. Ambient-Processed Colloidal Quantum Dot Solar Cells via Individual Pre-Encapsulation of Nanoparticles. *J. Am. Chem. Soc.* **2010**, *132*, 5952–5953.

(10) Pattantyus-Abraham, A. G.; Kramer, I. J.; Barkhouse, A. R.; Wang, X.; Konstantatos, G.; Debnath, R.; Levina, L.; Raabe, I.; Nazeeruddin, M. K.; Grätzel, M.; Sargent, E. H. Depleted-Heterojunction Colloidal Quantum Dot Solar Cells. *ACS Nano* **2010**, *4*, 3374–3380.

(11) Sze, S. M. *Physics of Semiconductor Devices*, 2nd ed.; John Wiley and Sons: New York, 1981.

(12) Hyun, B.-R.; Zhong, Y.-W.; Bartnik, A. C.; Sun, L.; Abruña, H. D.; Wise, F. W.; Goodreau, J. D.; Matthews, J. R.; Leslie, T. M.; Borrelli, N. F. Electron Injection from Colloidal PbS Quantum Dots into Titanium Dioxide Nanoparticles. *ACS Nano* **2008**, *2*, 2206–2212.

(13) Lee, H.; Leventis, H. C.; Moon, S.-J.; Chen, P.; Ito, S.; Haque, S. A.; Torres, T.; Nüesch, F.; Geiger, T.; Zakeeruddin, S. M.; Grätzel, M.; Nazeerruddin, M. K. PbS and CdS Quantum Dot-Sensitized Solid-State Solar Cells: "Old Concepts, New Results". *Adv. Funct. Mater.* **2009**, *19*, 2735–2742.

(14) Robel, I.; Kuno, M.; Kamat, P. V. Size-Dependent Electron Injection from Excited CdSe Quantum Dots into TiO_2 Nanoparticles. *J. Am. Chem. Soc.* **2007**, *129*, 4136–4137.

(15) Chang, C.-H.; Lee, Y.-L. Chemical Bath Deposition of CdS Quantum Dots Onto Mesoscopic TiO_2 Films for Application in Quantum-Dot-Sensitized Solar Cells. *Appl. Phys. Lett.* **2007**, *91*, 053503.

(16) Shalom, M.; Dor, S.; Rühle, S.; Grinis, L.; Zaban, A. Core/CdS Quantum Dot/Shell Mesoporous Solar Cells with Improved Stability and Efficiency Using an Amorphous TiO_2 Coating. *J. Phys. Chem. C* **2009**, *113*, 3895–3898.

(17) Larramona, G.; Choné, C.; Jacob, A.; Sakakura, D.; Delatouche, B.; Péré, D.; Cieren, X.; Nagino, M.; Bayón, R. Nanostructured Photovoltaic Cell of the Type Titanium Dioxide, Cadmium Sulfide Thin Coating, and Copper Thiocyanate Showing High Quantum Efficiency. *Chem. Mater.* **2006**, *18*, 1688–1696.

(18) Lee, H. J.; Chen, P.; Moon, S.-J.; Sauvage, F.; Sivula, K.; Bessho, T.; Gamelin, D. R.; Comte, P.; Zakeeruddin, S. M.; Seok, S. I.; Grätzel, M.; Nazeeruddin, M. K. Regenerative PbS and CdS Quantum Dot Sensitized Solar Cells with a Cobalt Complex as Hole Mediator. *Langmuir* **2009**, *25*, 7602–7608.

(19) Baker, D. R.; Kamat, P. V. Photosensitization of TiO_2 Nanostructures with CdS Quantum Dots: Particulate versus Tubular Support Architectures. *Adv. Funct. Mater.* **2009**, *19*, 805–811.

(20) Gónzalez-Pedro, V.; Xu, X.; Mora-Seró, I.; Bisquert, J. Modeling High-Efficiency Quantum Dot Sensitized Solar Cells. *ACS Nano* **2010**, *4*, 5783–5790.

(21) Lee, Y.-L.; Lo, Y.-S. Highly Efficient Quantum-Dot-Sensitized Solar Cell Based on Co-Sensitization of CdS/CdSe. *Adv. Funct. Mater.* **2009**, *19*, 604–609.

(22) Yang, S. M.; Huang, C. H.; Zhai, J.; Wang, Z. S.; Jiang, L. High Photostability and Quantum yield of Nanoporous TiO_2 Thin Film Electrodes Co-sensitized with Capped Sulfides. *J. Mater. Chem.* **2002**, *12*, 1459–1464.

(23) Lee, H. J.; Bang, J.; Park, J.; Kim, S.; Park, S.-M. Multilayered Semiconductor (CdS/CdSe/ZnS)-Sensitized TiO_2 Mesoporous Solar Cells: All Prepared by Successive Ionic Layer Adsorption and Reaction Processes. *Chem. Mater.* **2010**, *22*, 5636–5643.

(24) Vogel, R.; Hoyer, P.; Weller, H. Quantum-Sized PdS, CdS, Ag_2S, Sb_2S_3 and Bi_2S_3 Particles as Sensitizers for Various Nanoporous Wide-Bandgap Semiconductors. *J. Phys. Chem.* **1994**, *98*, 3183–3188.

(25) Fabregat-Santiago, F.; Mora-Seró, I.; Garcia-Belmonte, G.; Bisquert, J. Cyclic Voltammetry Studies of Nanoporous Semiconductors. Capacitive and Reactive Properties of Nanocrystalline TiO_2 Electrodes in Aqueous Electrolyte. *J. Phys. Chem. B* **2003**, *107*, 758–768.

(26) Mora-Seró, I.; Giménez, S.; Moehl, T.; Fabregat-Santiago, F.; Lana-Villareal, T.; Gómez, R.; Bisquert, J. Factors Determining the Photovoltaic Performance of a CdSe Quantum Dot Sensitized Solar Cell: the Role of the Linker Molecule and of the Counter Electrode. *Nanotechnology* **2008**, *19*, 424007.

(27) Barea, E. M.; Zafer, C.; Gultekin, B.; Aydin, B.; Koyuncu, S.; Icli, S.; Fabregat-Santiago, F.; Bisquert, J. Quantification of the Effects of Recombination and Injection in the Performance of Dye-Sensitized Solar Cells Based on N-Substituted Carbazole Dyes. *J. Phys. Chem. C* **2010**, *114*, 19840–19848.

(28) Fabregat-Santiago, F.; Bisquert, J.; Garcia-Belmonte, G.; Boschloo, G.; Hagfeldt, A. Influence of Electrolyte in Transport and Recombination in Dye-Sensitized Solar Cells Studied by Impedance Spectroscopy. *Sol. Energy Mater. Sol. Cells* **2005**, *87*, 117–131.

(29) Bisquert, J.; Fabregat-Santiago, F.; Mora-Seró, I.; Garcia-Belmonte, G.; Giménez, S. Electron Lifetime in Dye-Sensitized Solar Cells: Theory and Interpretation of Measurements. *J. Phys. Chem. C* **2009**, *113*, 17278–17290.

(30) Barea, E. M.; Shalom, M.; Giménez, S.; Hod, I.; Mora-Seró, I.; Zaban, A.; Bisquert, J. Design of Injection and Recombination in Quantum Dot Sensitized Solar Cells. *J. Am. Chem. Soc.* **2010**, *132*, 6834–6839.

(31) Shalom, M.; Rühle, S.; Hod, I.; Yahav, S.; Zaban, A. Energy Level Alignment in CdS Quantum Dot Sensitized Solar Cells Using Molecular Dipoles. *J. Am. Chem. Soc.* **2009**, *131*, 9876–9877.

(32) Bisquert, J.; Mora-Seró, I. Simulation of Steady-State Characteristics of Dye-Sensitized Solar Cells and the Interpretation of the Diffusion Length. *J. Phys. Chem. Lett.* **2010**, *1*, 450–456.

(33) Mora-Seró, I.; Bisquert, J. Breakthroughs in the Development of Semiconductor-Sensitized Solar Cells. *J. Phys. Chem. Lett.* **2010**, *1*, 3046–3052.

(34) O'Regan, B. C.; Durrant, J. R.; Sommeling, P. M.; Bakker, N. J. Influence of the $TiCl_4$ Treatment on Nanocrystalline TiO_2 Films in Dye-Sensitized Solar Cells. 2. Charge Density, Band Edge Shifts, and Quantification of Recombination Losses at Short Circuit. *J. Phys. Chem. C* **2007**, *111*, 14001–14010.

(35) Giménez, S.; Mora-Seró, I.; Macor, L.; Guijarro, N.; Lana-Villarreal, T.; Gómez, R.; Diguna, L. J.; Shen, Q.; Toyoda, T.; Bisquert, J. Improving the Performance of Colloidal Quantum Dot Sensitized Solar Cells. *Nanotechnology* **2009**, *20*, 295204.

(36) Shen, Q.; Kobayashi, J.; Diguna, L. J.; Toyoda, T. Effect of ZnS Coating on the Photovoltaic Properties of CdSe Quantum Dot-Sensitized Solar Cells. *J. Appl. Phys.* **2008**, *103*, 084304.